



ELSEVIER

12 March 1998

PHYSICS LETTERS B

Physics Letters B 422 (1998) 334–338

Improved limit on the branching ratio of $\mu^- \rightarrow e^+$ conversion on titanium

SINDRUM II Collaboration

J. Kaulard^a, C. Dohmen^a, H. Haan^a, W. Honecker^a, D. Junker^a, G. Otter^a,
M. Starlinger^a, P. Wintz^{a,1}, J. Hofmann^b, W. Bertl^c, J. Egger^c, B. Krause^c,
S. Eggli^d, R. Engfer^d, Ch. Findeisen^d, E.A. Hermes^d, T. Kozlowski^{d,2},
C.B. Niebuhr^{d,3}, M. Rutsche^d, H.S. Pruys^d, A. van der Schaaf^{d,4}

^a III. Physikalisches Institut B der RWTH Aachen, D-52056 Aachen, Germany

^b Institut für Teilchenphysik der ETH Zürich, CH-5232 Villigen PSI, Switzerland

^c Paul Scherrer Institut, CH-5232 Villigen PSI, Switzerland

^d Physik-Institut der Universität Zürich, CH-8057 Zürich, Switzerland

Received 18 September 1997; revised 14 October 1997

Editor: K. Winter

Abstract

The SINDRUM II spectrometer at PSI is used in searches for $\mu \rightarrow e$ conversion in muonic atoms. Here we report on a search for the charge-changing $\mu^- \rightarrow e^+$ conversion on titanium. The measurements yielded the new upper limits $\Gamma(\mu^- \text{Ti} \rightarrow e^+ \text{Ca}^{GS})/\Gamma(\mu^- \text{Ti capture}) < 1.7 \times 10^{-12}$ (90% CL) for the ground state transition and $\Gamma(\mu^- \text{Ti} \rightarrow e^+ \text{Ca}^{GDR})/\Gamma(\mu^- \text{Ti capture}) < 3.6 \times 10^{-11}$ (90% CL) for a giant dipole resonance excitation with both a mean energy and a width of 20 MeV. These results improve on our previous best limits by a factor of 2.5. © 1998 Elsevier Science B.V.

PACS: 13.35.Bv; 14.60.-z; 36.10.Dr

Within the Standard Model the only flavour-changing mechanism is CKM mixing in the quark eigenstates. Since neutrino mass degeneracy pre-

cludes this mechanism in the leptonic sector the three lepton flavours are separately conserved, in agreement with all present observations. In most extensions of the model this need not be true and lepton-flavour violation might well give the first hint of physics beyond the Standard Model. From the many tests of lepton-flavour conservation coherent $\mu^- \rightarrow e^-$ conversion gives the best constraints in a large variety of models [1–3].

Total lepton number need not be conserved either

¹ Present address: Physik-Institut der Universität Zürich, CH-8057 Zürich, Switzerland.

² Permanent address: Institute for Nuclear Studies, PL-05-400 Swierk, Poland.

³ Present address: DESY, D-22607 Hamburg, Germany.

⁴ E-mail: VANDERSCHAAF@PSI.CH.

allowing processes like neutrinoless double β -decay or charge-changing $\mu \rightarrow e$ conversion, $\mu^-(Z, A) \rightarrow e^+(Z-2, A)$. Both require relatively complex mechanisms involving two nucleons. Recent estimates of the latter process resulted in values for the branching ratio which could be as large as $\mathcal{O}(10^{-12})$ for a supersymmetric model with R-parity breaking [4] or $\mathcal{O}(10^{-14})$ for a left-right symmetric model [5]. Since the nucleus changes from initial to final state there is no coherent enhancement of the ground state (GS) transition, as in the case of $\mu^- \rightarrow e^-$ conversion. Usually one assumes a giant dipole resonance (GDR) for the daughter nucleus with both a mean energy and a width of 20 MeV resulting in a broad momentum distribution for the emitted positron.

Background results from radiative muon capture (RMC) and pion capture (RPC), followed by asymmetric e^+e^- production in the target and from cosmic rays. The RMC background has an endpoint which is about 10 MeV below the kinematic endpoint (see below). RPC background should be kept under control by minimizing the pion contamination of the beam and by rejecting events in prompt coincidence with a beam counter. The vast majority of cosmic ray background events can be recognized by the occurrence of additional detector signals.

The measurement was done at the μ E1 beam line at PSI. Detailed information can be found in Ref. [6]. The SINDRUM II spectrometer consists of a set of concentric cylindrical detectors inside a superconducting solenoid (Fig. 1). The muons enter the setup axially and traverse a CH_2 moderator, a plastic beam counter of 3.2 g/cm^2 overall thickness and a second moderator before reaching the target at the center. The purpose of this second moderator is to stop more than 99% of the pions reaching it. The resulting π/μ ratio in the target stops is $\approx 10^{-7}$. The target is made of titanium foil with a thickness $23.8 \mu\text{m}$. The foil is arranged symmetrically with respect to the beam axis with an $x-y$ cross section resembling a flower with 80 petals. The target has a length of 300 mm, an outer radius of 81 mm and a total mass of 427 g.

The cylindrical tracking region has a diameter of 1.3 m and a length of 1.5 m. At the field strength of 1.2 T all charged particles leaving the target with transverse momenta below $100 \text{ MeV}/c$ are contained radially inside this region. Starting from the

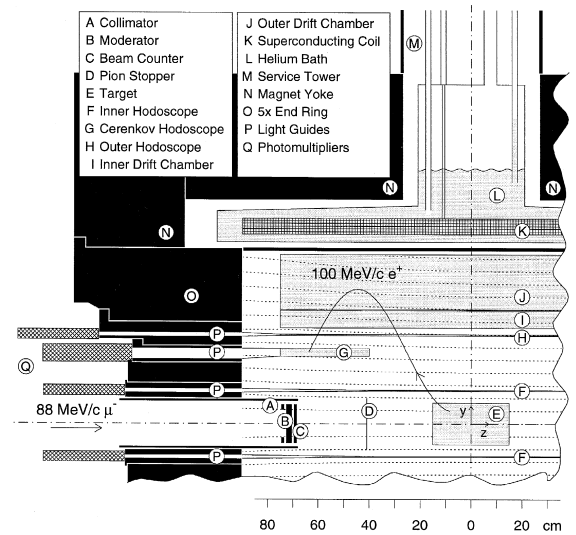


Fig. 1. Cross section through SINDRUM II. See the text for a discussion of the various detector components. The dashed lines represent the magnetic field lines. The Cartesian coordinate system is indicated at the spectrometer center.

target they traverse (i) at a radial distance of $r = 130$ mm an inner plastic scintillator hodoscope with 32 strips of 3 mm thickness and 800 mm length, (ii) at $r = 349$ mm an outer plastic scintillator hodoscope with 64 strips of 5 mm thickness and 1.5 m length, (iii) between 376 mm and 445 mm the radial drift chamber DC1, (iv) between 449 mm and 648 mm the radial drift chamber DC2, and (v) at $r = 285$ mm, on both ends of the tracking region, two Čerenkov hodoscopes, each with 16 lucite elements of 30 mm thickness and 350 mm length. The particles of interest cross the drift region of DC1 at least twice before reaching one of the two Čerenkov hodoscopes.

DC1 [7] is filled with $\text{CO}_2/\text{iC}_4\text{H}_{10}$ (70/30), a slow drift gas with a Lorentz deflection angle of only 6° at 1.2 T. The sense wire plane is close to the outer wall, which is covered with 4.4 mm wide cathode strips at $\pm 72^\circ$ relative to the wires. The cathode signals are used to determine the position of the hits along the sense wires. The cathode strips start at $z = 0$ mm with an orientation opposite to the e^- trajectories to give optimal performance for $\mu^- \rightarrow e^-$ conversion. As a consequence positrons may cross only few cathode strips resulting in a reduced reconstruction efficiency (see below). DC2 is filled with

Table 1

Endpoint energies for $\mu^- \rightarrow e^+$ conversion and radiative muon capture for the various titanium isotopes

A	abundance (%)	$E_{\mu^- e^+}^{\max}$ (MeV)	E_{RMC}^{\max} (MeV)
46	7.94	102.26	91.4 ± 2.0
47	7.44	100.66	93.2 ± 2.0
48	73.78	98.99	89.7 ± 2.0
49	5.51	95.98	91.8 ± 2.0
50	5.34	91.39	86.9 ± 2.0

He/iC₄H₁₀ (88/12) with a radiation length of 1140 m.

The spectrometer response to $\mu^- \rightarrow e^+$ conversion and RMC was obtained by simulation [8]. The reliability of the simulation was checked for 69.8 MeV/c positrons from the decay $\pi^+ \rightarrow e^+ \nu_e$ in a reduced magnetic field of 0.85 T. The photon energy spectrum observed for RMC on ⁴⁰Ca can be described by Primakoff's formula [9] with an empirical endpoint of $E_{RMC}^{\max} = 93 \pm 2$ MeV [10], well below the kinematical endpoint of 102.5 MeV. We assume the same shift for RMC on the various titanium isotopes. The resulting values are compared with the $\mu^- \rightarrow e^+$ endpoint energies in Table 1. The yield has been normalized to the calcium data after correction for the empirical 1/Z dependence [11].

The muon channel was tuned to a momentum band of 88.0 ± 4.5 MeV/c. The beam intensity was $1.15 \times 10^7 \mu^- s^{-1}$ for a mean proton current of 0.5 mA. The fraction of muons stopping in the target was $61.6 \pm 0.3\%$, as determined with the help of an additional beam counter at the spectrometer exit. The total number of muons stopping in the target during the effective measuring period of 60 days was $(2.95 \pm 0.13) \cdot 10^{13}$. Given the 85% probability for ordinary muon capture in titanium, these gave rise to a total number of $N_{OMC} = (2.52 \pm 0.11) \cdot 10^{13}$ captured muons. Cosmic ray background was studied in beam-off periods.

The trigger for data readout was based on the $x - y$ hit pattern from the outer hodoscope and DC1. In addition signals in the inner hodoscope and a Čerenkov hodoscope were required. A total of $4 \cdot 10^6$ electron and positron events were recorded.

In the off-line event reconstruction helical trajectories were searched and the momentum was fitted to

the first two DC1 track elements. Inhomogeneities of the magnetic field in the order of 10% (see Fig. 1) have been taken into account. The reconstruction efficiency for positrons from the target was 0.55 ± 0.10 . Most of the losses result from the low efficiency of the DC1 cathodes for positron trajectories. The resulting positron sample contains 2550 events with a momentum above 80 MeV/c. Due to a $\approx 0.2\%$ probability of charge misidentification and since there are almost hundred times more electrons than positrons this sample is contaminated by $\approx 20\%$ misidentified electrons.

Half of the events show a prompt signal in the beam counter trace, which has been recorded with a wave-form digitizer. These events are caused by RPC and misidentified scattered beam electrons and have been removed by a 20 ns wide prompt veto. The relatively large width, caused by the large spread in the flight time of low-energy pions from the second moderator to the target, results in an efficiency loss of 0.24 ± 0.01 for muonic-atom decays. The remaining sample is dominated by cosmic ray background, which usually can be recognized by the occurrence of additional signals in the detectors. Removal of these events leads to a sample of 290 events at the cost of a 6% efficiency loss for muonic-atom decays.

The final positron sample has a linear momentum distribution with an endpoint around 92.3 MeV/c (see Fig. 2a) with an isolated candidate event at 95.7 MeV/c. Also shown in Fig. 2a are the distributions resulting from the $\mu^- \rightarrow e^+$ simulations for the GS and GDR final states. The momentum distribution from the beam-off periods (see Fig. 2c), which correspond to about the same effective measuring time, shows one event in the region of interest as well. The isolated event can thus be explained by cosmic ray background and no evidence is found for $\mu^- \rightarrow e^+$ conversion.

The final sample of 290 events still contains some misidentified scattered beam electrons which were not recognized by the beam counter. These prompt events have a well-defined time correlation with the proton bunches of the cyclotron which results in a peak in the distribution of the phase φ_{rf} of the decay time relative to the 50.63 MHz radio frequency signal of the cyclotron (see insert Fig. 2b). 194 events with $|\varphi_{rf}| > 2$ ns have been interpreted as purely

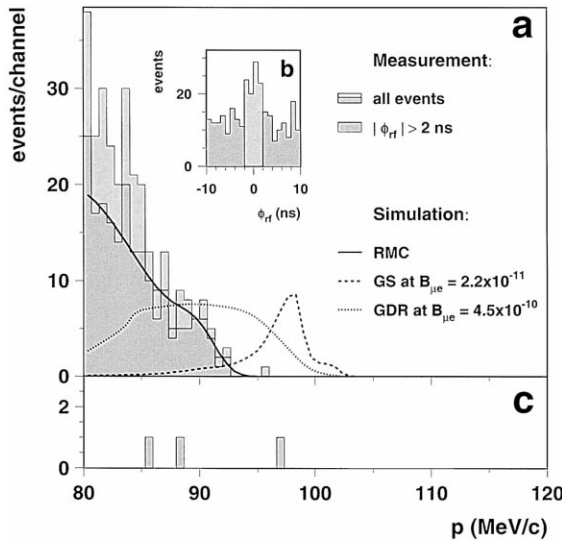


Fig. 2. Positron momentum distributions for measuring periods with (a,b) and without (c) muon beam. The measured distribution in part a is compared with the *GS* and *GDR* expectations for $\mu^- \rightarrow e^+$ conversion. The insert b shows the distribution of ϕ_{rf} , the decay time relative to the 50.63 MHz cyclotron frequency, exhibiting a peak caused by misidentified scattered beam electrons. The events from the grey region outside the peak have been interpreted as *RMC* events. Their momentum distribution is compared with the results from the *RMC* simulation discussed in the text.

RMC. Their momentum spectrum (also shown in Fig. 2a) can not be reproduced assuming the photon distribution discussed above: the measured distribution reaches 3 MeV beyond the E_{RMC}^{\max} value of the dominant isotope (see Table 1). The agreement demonstrated in Fig. 2a, was obtained by including an additional component with a 93 MeV endpoint, corresponding to the maximum photon energy in the reaction $^{48}\text{Ti}(\mu^-, \nu_\mu \gamma)^{48}\text{Sc}(0^+, 6.68 \text{ MeV})$. Such a weak transition to a discrete final state could not have been resolved in the available *RMC* data. The number of positrons thus obtained from the Primakoff continuum is 118 ± 15 , in nice agreement with the 130 ± 44 events expected from the *RMC* simulation.

The upper limit for the $\mu^- \rightarrow e^+$ branching ratio has been calculated using

$$B_{\mu^- e^+}^i < \frac{n_{\mu^- e^+}^{\max}}{N_{OMC} \cdot A_{\mu^- e^+}^i \cdot \epsilon_{\mu^- e^+}^i}, \quad i = GS, GDR \quad (1)$$

with $n_{\mu^- e^+}^{\max}$ the upper limit on the observed number of $\mu^- \rightarrow e^+$ events, N_{OMC} the total number of ordinary muon captures discussed above, $A_{\mu^- e^+}^i$ the geometric acceptance and $\epsilon_{\mu^- e^+}^i$ the product of all efficiency factors, which account for the losses in the detector signals, readout trigger, data acquisition and event reconstruction and selection. Following [12] the uncertainties in N_{OMC} , $A_{\mu^- e^+}^i$ and $\epsilon_{\mu^- e^+}^i$ have been taken into account in the value of $n_{\mu^- e^+}^{\max}$:

$$n_{\mu^- e^+}^{\max} = n^0 \left(1 + \frac{n^0(n^0 + n_b - n_o)}{2(n^0 + n_b)} r^2 \right),$$

with: n^0 the value of $n_{\mu^- e^+}^{\max}$ in the absence of any uncertainty, r the relative uncertainty of $N_{OMC} \cdot A_{\mu^- e^+}^i \cdot \epsilon_{\mu^- e^+}^i$, n_b the expected number of background events and n_o the observed number of events.

Using the prescription described in Ref. [13] for $n_o = 1$ and $n_b = 1$, $n^0 = 3.3$ at 90% confidence level. Table 2 lists the values of $A_{\mu^- e^+}$ and the various efficiencies for *GS* and *GDR* separately. The effect of the 92.3 MeV/c momentum threshold has been absorbed in $A_{\mu^- e^+}$. Detector inefficiencies and dead-time in the trigger logic and the data acquisition system are included in the trigger efficiency $\epsilon_{trigger}$. Using these values Eq. 1 yields the following upper limits:

$$B_{\mu^- e^+}^{GS} < 1.7 \cdot 10^{-12} \quad (90\% \text{ CL})$$

$$B_{\mu^- e^+}^{GDR} < 3.6 \cdot 10^{-11} \quad (90\% \text{ CL})$$

which improve on the previous results [14] by a factor of 2.5.

Meanwhile first data-taking has started at a new dedicated beamline at PSI. This channel delivers a high-purity muon beam which no longer requires any beam veto to control background from *RPC* or

Table 2

Spectrometer acceptance and some efficiency factors for a momentum threshold of 92.3 MeV/c

	ground state	giant resonance
$A_{\mu^- e^+}$	0.298 ± 0.004	0.0137 ± 0.0003
$\epsilon_{trigger}$	0.71 ± 0.02	0.74 ± 0.02
ϵ_{reco}	0.55 ± 0.10	0.55 ± 0.10
ϵ_{cuts}	0.71 ± 0.07	0.69 ± 0.07
$\epsilon_{\mu^- e^+}$	0.28 ± 0.06	0.28 ± 0.06
$A_{\mu^- e^+} \cdot \epsilon_{\mu^- e^+}$	0.083 ± 0.016	0.0038 ± 0.0007

scattered electrons. Thanks to increased beam intensity a further improvement in sensitivity by roughly one order of magnitude is expected.

This work was supported in part by the Bundesministerium für Bildung, Wissenschaft, Forschung und Technologie, Germany, under contract number 06AC651 and by the Swiss National Science Foundation.

References

- [1] J.D. Vergados, *Phys. Rep.* 133 (1986) 1.
- [2] A. van der Schaaf, in: A. Faessler (Ed.), *Progress in Particle and Nuclear Physics*, vol. 31, Pergamon, Oxford, 1993, p. 1.
- [3] P. Depommier, C. Leroy, *Rep. Prog. Phys.* 58 (1995) 61.
- [4] K.S. Babu, R.N. Mohapatra, in: Ejiri, Kishimoto, Sato (Eds.), *Proceedings of WEIN95*, World Scientific, Singapore, 1995, pp. 212–216.
- [5] R.N. Mohapatra, in: A. Faessler (Ed.), *Progress in Particle and Nuclear Physics*, vol. 31, Pergamon, Oxford, 1993, p. 39.
- [6] J.Q. Kaulard, Ph.D. thesis, RWTH Aachen, 1997.
- [7] M. Grossmann-Handschin et al., *Nucl. Instr. Meth. A* 327 (1993) 378.
- [8] GEANT, CERN Program Library Long Write-up W5013, Geneva, Switzerland, 1993.
- [9] H. Primakoff, *Rev. Mod. Phys.* 31 (1959) 802.
- [10] D.S. Armstrong et al., *Phys. Rev. C* 46 (1992) 1094.
- [11] M. Gmitro, P. Truoel, *Adv. in Nucl. Phys.* 18 (1987) 241.
- [12] R.D. Cousins, V.L. Highland, *Nucl. Instr. Meth. A* 320 (1992) 331.
- [13] Particle Data Group, *Phys. Rev. D* 54 (1996) 1.
- [14] SINDRUM II Collaboration, C. Dohmen et al., *Phys. Lett. B* 317 (1993) 631.